The Astrophysical Journal, 863:188 (8pp), 2018 August 20 https://doi.org/10.3847/1538-4357/aad3cf

Magnetic Mirroring and Focusing of Cosmic Rays

Kedron Silsbee[1], Alexei V. Ivlev[1], Marco Padovani[2], and Paola Caselli[1]
[1] Max-Planck-Institut für Extraterrestrische Physik, D-85748 Garching, Germany; ksilsbee@mpe.mpg.de, ivlev@mpe.mpg.de
[2] INAF–Osservatorio Astrofisico di Arcetri, Largo E. Fermi 5, I-50125 Firenze, Italy
Received 2018 May 13; revised 2018 July 11; accepted 2018 July 12; published 2018 August 23

Abstract

We study the combined impact of magnetic mirroring and focusing on the ionization by cosmic rays (CRs) in dense molecular clouds and circumstellar disks. We show that for effective column densities of up to $\sim 10^{25}$ cm^{-2} (where ionization is the main mechanism of energy loss by CRs) the two effects practically cancel each other out, provided the magnetic field strength has a single peak along field lines. In this case the ionization rate at a given location is controlled solely by attenuation of interstellar CRs due to energy losses. The situation is very different in the presence of magnetic pockets—local minima of the field strength, where the CR density and thus ionization can be reduced drastically. We obtain simple analytical expressions allowing accurate calculation of the ionization rate in these regions.

Key words: cosmic rays – ISM: clouds – plasmas

1. Introduction

The ionization degree of molecular clouds is a critical factor in the dynamics of star formation. A small fraction of ionized species controls the coupling of the Galactic magnetic field to the predominantly neutral gas of the cloud, influencing its stability against gravitational collapse (Mestel & Spitzer 1956), the efficiency of the fragmentation process (Price & Bate 2008), and the formation of circumstellar disks around young stars (Allen et al. 2003). The main source of ionization in dark regions of molecular clouds and pre-stellar cores is cosmic rays (CRs), which initiate a chain of chemical reactions starting from the collisional ionization of the most abundant species, molecular hydrogen (Yamamoto 2017).

CRs, responsible for the ionization in dense cores and circumstellar disks, propagate along the local magnetic field. The magnetic configuration in such objects can be very complicated (Joos et al. 2012; Li et al. 2013; Padovani et al. 2013), and the field strength can be much larger than the interstellar value (Crutcher 2012). The field strength increases along the field lines converging into denser central regions, which leads to efficient mirroring of the penetrating CRs—their pitch angles increase in response to the growing field until reaching 90°, and thus more and more particles are reflected back. On the other hand, the convergence of field lines results in the CR focusing. These two competing effects play important roles in various processes occurring in molecular clouds (Cesarsky & Völk 1978; Ko 1992; Chandran 2000; Desch et al. 2004; Padoan & Scalo 2005).

Recently, there have been studies (Padovani & Galli 2011; Padovani et al. 2013) investigating the combined effect of magnetic mirroring and focusing on the CR ionization in the dense molecular cores. A comprehensive analysis of the CR propagation in static and collapsing magnetized clouds has been carried out, by varying the relative strength of the toroidal/poloidal field components and the mass-to-flux ratio. The authors concluded that mirroring always dominates over focusing, implying a reduction of the CR ionization rate by a factor of about 2–3 with respect to the case where these magnetic effects are neglected. It was also shown that, for large values of the flux-to-mass ratio, these effects reduce the ionization in collapsing clouds by more than an order of magnitude, which can have important consequences for the dynamical evolution and the formation of disks (e.g., Zhao et al. 2018).

The major aim of the present work is to perform a general analysis of the effects of CR mirroring and focusing in dense cores and circumstellar disks. We identify universal mechanisms that govern the CR ionization in such environments, assuming that there is no stochastic change in the pitch angle. This assumption is well justified, since the field structure normally remains stationary at a timescale of CR crossing (the physical velocity of CRs is typically a few orders of magnitude larger than the velocity of MHD waves).[3] We also make use of the fact that the small-scale resonant MHD turbulence, which could lead to efficient CR scattering, is completely damped under such conditions due to frequent ion-neutral collisions (e.g., Ivlev et al. 2018).

In Section 2, we study the net effect of the mirroring and focusing on the CR density when energy losses are negligible; we identify two distinct cases, of single- and multiple-peaked magnetic field strength, and demonstrate that in the former case the mirroring and focusing cancel out exactly, while in the latter case a drastic reduction of the CR density is possible. In Section 3, we determine the exact upper and lower bounds for the ionization rate in the two cases; we show that ionization is practically unaffected for a single-peaked field and is reduced for a multiple-peaked field, and provide analytical expressions for the ionization rate. Finally, in Section 4, we summarize our main findings and briefly discuss implications for the relevant astrophysical problems.

2. Mirroring and Focusing without Losses

Consider the magnetic field threading a molecular cloud or circumstellar disk (below we use the term "cloud"), as sketched in Figure 1(a). Let s be the distance coordinate along a field line, and assume that outside the cloud there is a constant

[3] Fast processes associated with possible magnetic reconnection (see, e.g., Lazarian 2014), induced in these dense regions by rotationally driven MHD turbulence, require separate consideration, which is beyond the scope of this paper.

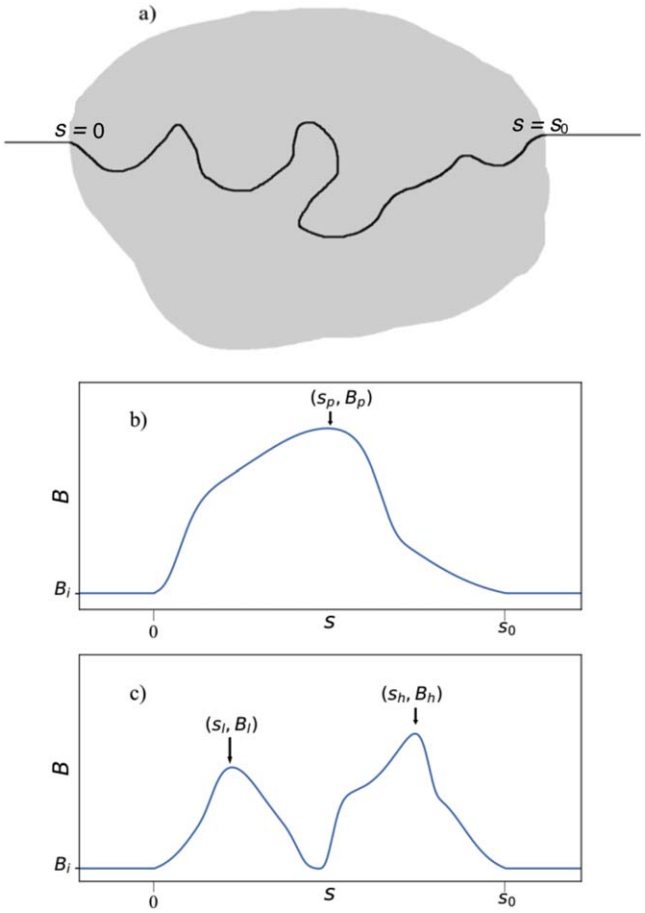

Figure 1. Panel (a) shows a sketch of a magnetic field line entering a cloud (gray region). Panels (b) and (c) depict sketches of the magnetic field strength B as a function of distance s along a field line. Panel (b) shows the single-peaked case discussed in Section 2.1; panel (c) shows the double-peaked case discussed in Section 2.2.

(interstellar) field strength B_i. The cloud is surrounded by the interstellar medium with isotropically distributed CRs that can travel in both directions without energy losses, along any field line that penetrates the cloud.

In the absence of scattering processes, the pitch angle α (between the velocity of a CR particle and the field) satisfies the relation

$$\frac{\sin^2\alpha}{B(s)} = \frac{\sin^2\alpha_i}{B_i}, \tag{1}$$

which follows from the adiabatic invariance of the magnetic moment of a particle (e.g., Chen 1974). In this case, the steady-state kinetics of CRs with given momentum p is characterized by the distribution function $f(\mu, p, s)$,[4] obeying the equation (Morfill et al. 1976; Cesarsky & Völk 1978)

$$\mu\frac{\partial f}{\partial s} - (1-\mu^2)\frac{d\ln\sqrt{B}}{ds}\frac{\partial f}{\partial \mu} = 0, \tag{2}$$

where $\mu \equiv \cos\alpha$. A general solution of this equation is any function of $(1-\mu^2)/B(s)$, showing that the CR distribution is conserved for a given magnetic moment. This conclusion, which naturally follows from the Liouville theorem, implies

$$f(\mu, s) = f_i(\mu_i), \tag{3}$$

where $f_i(\mu_i)$ is the distribution function of interstellar CRs. The local value of μ is determined from Equation (1),

$$\mu(\mu_i, s) = \pm\sqrt{1 - \tilde{B}(s)(1-\mu_i^2)}, \tag{4}$$

where $\tilde{B}(s) = B(s)/B_i$ is the magnetic "focusing factor" (increasing B implies the proportional focusing of field lines). A monotonic increase of the magnetic field strength leads to the particle mirroring: interstellar CRs can reach the position s only if $\sin\alpha_i \leqslant 1/\sqrt{\tilde{B}(s)}$, i.e., if $|\mu_i| \geqslant \sqrt{1 - 1/\tilde{B}(s)}$.

Equation (3) has a simple physical meaning. Using the relation

$$\frac{\partial\mu}{\partial\mu_i} = \tilde{B}(s)\frac{\mu_i}{\mu}, \tag{5}$$

we obtain $f(\mu, s)\mu\ \delta\mu = \tilde{B}(s) f_i(\mu_i)\mu_i\ \delta\mu_i$. Written in this form, the equation expresses a conservation of the *differential flux* along a field line, taking into account that the pitch angle varies with s in accordance with Equation (1) and that the local particle density is proportional to the focusing factor $\tilde{B}(s)$.

2.1. Single Maximum of the Field Strength

In this section, we assume that $B(s)$ has only one peak on the interval $0 \leqslant s \leqslant s_0$, located at s_p, as shown in Figure 1(b). Consider CRs at $0 < s < s_p$ moving in the $+s$ direction (referred to as *forward-moving particles*), and denote their local distribution by f_+. Since B (and thus α) continuously increase for such particles, f_+ is nonzero for all values of μ between 0 and 1.

Let us calculate the local differential density (per unit momentum) of forward-moving CRs, $n_+(p, s) = \int_0^1 f_+\, d\mu$. Using Equation (3), we substitute $f_+ = f_i$ and keep in mind that the distribution of interstellar CRs is isotropic, $f_i = \frac{1}{2}n_i$, where $n_i(p)$ is their differential density. Then the integration over μ yields $n_+ = \frac{1}{2}n_i$. Thus, the density of forward-moving particles remains constant and equal to the density of CRs entering the cloud from the left.

Local CRs also include particles that are moving in the $-s$ direction (*backward-moving particles*). Their distribution f_- is a sum of two components: particles with $-\mu_p < \mu < 0$, which were mirrored before reaching the peak at $s = s_p$, and particles with $-1 \leqslant \mu < -\mu_p$, which passed through the peak from the other side.[5] Taking into account that $f_-(\mu, s) = f_+(|\mu|, s)$ for the mirrored particles and using Equation (3) for both components, we obtain $f_- = f_i$ and hence $n_- = \frac{1}{2}n_i$.

We conclude that the effects of magnetic mirroring and focusing cancel exactly when energy losses by CRs are neglected (i.e., when Equation (2) holds). The distribution of particles does not depend on the location in a cloud and coincides with the distribution of interstellar CRs, f_i (Cesarsky & Völk 1978). For nonrelativistic CRs, the latter is isotropic to a very high degree, and therefore the local density is equal to

[4] For brevity, below we only show arguments of f that are essential for understanding. We use the normalization such that total number density of CRs is $\int dp \int f\ d\mu$.

[5] The value of $\mu_p = \sqrt{1 - B/B_p}$ is derived from Equation (4) by substituting $1 - \mu_i^2 = 1/\tilde{B}_p$; the latter follows from the mirroring condition ($\mu = 0$) at the peak.

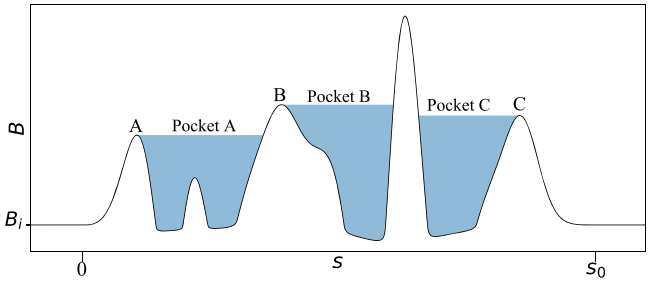

Figure 2. Situation where the magnetic field has multiple maxima along the field line. This results in multiple magnetic pockets, indicated by the shading.

the density of CRs outside the cloud, n_i. We note, however, that if $f_i(\mu_i)$ exhibits anisotropy (Parker 1963), the density is not conserved—it generally increases (decreases) with s if f_i has a maximum (minimum) at $|\mu_i| \approx 1$: for example, a beam concentrated near $|\mu_i| \approx 1$ is practically not mirrored, so the focusing leads to the density increase; on the contrary, particles with a completely depleted distribution near $|\mu_i| \approx 1$ are totally mirrored when they reach a location where the field is sufficiently strong.

2.2. Multiple Maxima

If the magnetic field strength has more than one maximum along a field line, then the focusing factor is still $\tilde{B}(s)$, but the calculation of the mirroring effect is different. Therefore, the particle density is no longer constant along that field line, as shown below.

Suppose first that $B(s)$ has a "lower" peak B_l at $s = s_l$ and a "higher" peak B_h at $s = s_h$, as in Figure 1(c). If either $B(s) \geqslant B_l$, or s is not between the two peaks, the "lower" peak has no effect on the local particle density, and the results from Section 2.1 are applicable. A more interesting situation occurs in a *magnetic "pocket,"* for $s_l < s < s_h$ and $B(s) < B_l$. In this case there are three groups of particles contributing to the local density: particles moving in the $-s$ direction that came from $s > s_0$ and passed through the maximum in B at s_h; particles moving in the $+s$ direction that came from $s < 0$ and passed through the maximum in B at s_l; and finally those that came from $s < 0$, passed through s_l, but were reflected before reaching s_h and are now moving in the $-s$ direction.

The contribution of the first (backward-moving) group is calculated by integrating f_i over $-1 \leqslant \mu < -\mu_h$, with $\mu_h = \sqrt{1 - B/B_h}$ (see Section 2.1), which yields the density $\frac{1}{2}n_i(1 - \mu_h)$. This result does not depend on the direction of propagation, and therefore the contribution of the second (forward-moving) group can be obtained from the same expression by replacing μ_h with μ_l. The density of the third group of particles is not affected by their reflection, and thus is calculated by integrating over $\mu_l < \mu < \mu_h$, which yields $\frac{1}{2}n_i(\mu_h - \mu_l)$. Adding up the three contributions, we find the local density,

$$\frac{n(s)}{n_i} = 1 - \sqrt{1 - \frac{B(s)}{B_l}}. \qquad (6)$$

We see that n/n_i does not depend on B_h and is very sensitive to B_l. For example, a 1% reduction in B from the "lower" peak value, i.e., $B/B_l = 0.99$, leads to a 10% reduction of the local density.

This result can be straightforwardly generalized for the case of several peaks. Figure 2 illustrates such a situation, with magnetic pockets indicated by shading. From the same line of arguments as above it follows that the local density in *each* pocket is described by Equation (6), where B_l should be replaced by the respective value of the peak field (B_A, B_B, and B_C for pockets A, B, and C). We notice that Equation (6) remains applicable even if $B(s)$ has small peaks inside a pocket (as, e.g., for pocket A).

3. Effect of the Mirroring and Focusing on the Ionization Rate

In Section 2, we neglected energy losses by CRs and showed that in this case the magnetic mirroring and focusing exactly cancel each other out, if we assume the field strength has a single peak along field lines. In particular, this implies that the ionization in a cloud is not influenced by the magnetic effects as long as energy losses do not substantially attenuate CRs (specifically, do not modify the part of their energy spectrum providing the main contribution to the ionization, see discussion in Section 3.1). Then, irrespective of the strength and configuration of the magnetic field in the cloud, the ionization rate can be calculated using the density of interstellar CRs (i.e., as if the field strength inside the cloud remains constant and equal to B_i).

When the CR attenuation caused by energy losses cannot be neglected, two factors complicate the simple argument presented above. On the one hand, the density of forward-moving particles for $dB/ds > 0$ becomes *higher* compared to that in the constant-field case: the pitch angle of such particles continuously increases, which means that (for a given value of local pitch angle) they have shorter helical trajectories and therefore suffer *less attenuation*. On the other hand, the density of backward-moving mirrored particles is reduced at a given point, as they have traveled through more columns than those that are still forward-moving. Furthermore, the density of backward-moving particles passed through the cloud from the other side is more attenuated than that of forward-moving particles (unless we consider the central region of the cloud, where mirroring is less important and particles come from both sides with a similar attenuation).

To quantify the effect of the mirroring and focusing on the CR ionization, in Section 3.1, we first put bounds on the relative increase in the rate of ionization by forward-moving particles, assuming the field strength has a single peak. Then, in Section 3.2, we estimate the ratio of the ionization due to the mirrored particles to the ionization due to the forward-moving particles. Finally, in Section 3.3, we calculate a reduction of the ionization rate in magnetic pockets.

3.1. Ionization by the Forward-moving Particles

In the presence of continuous energy losses by CRs, the distribution function is described by the following steady-state kinetic equation (Skilling & Strong 1976; Cesarsky & Völk 1978):

$$v\mu\frac{\partial f}{\partial s} - v(1 - \mu^2)\frac{d\ln\sqrt{B}}{ds}\frac{\partial f}{\partial \mu} + \frac{\partial}{\partial p}(\dot{p}_{\rm loss} f) = 0, \qquad (7)$$

which is obtained by adding a loss term to Equation (2) (multiplied by the particle velocity v). The loss term is

characterized by the momentum decrease of a particle per unit time due to inelastic processes, $\dot{p}_{\rm loss} < 0$.

For further analysis it is convenient to use the particle kinetic energy E instead of the momentum p. Taking into account that $dE = v\ dp$, we obtain that the respective distributions are related via $f(\mu, p, s) = v(E)\hat{f}(\mu, E, s) \equiv j(\mu, E, s)$, where j is the so-called energy spectrum of CRs (and $\int \hat{f}\ d\mu$ is the differential density per unit energy). One can write the losses due to interaction with gas particles in the form $\dot{p}_{\rm loss} = -n_g(s)L(E)$, where n_g is the local gas number density and L is the loss function depending solely on the kinetic energy. Then, replacing μ with the new variable $(1 - \mu^2)/B(s)$ reduces Equation (7) to

$$\frac{\hat{\mu}}{n_g}\frac{\partial j}{\partial s} - \frac{\partial}{\partial E}(Lj) = 0, \tag{8}$$

where $\hat{\mu}(\mu_i, s)$ denotes a function of position for given μ_i, as determined by Equation (4).

We point out that Equation (8) can be used as long as losses do not result in a substantial scattering of a CR particle along its path (otherwise, a term describing the pitch-angle diffusion should be added, see Morfill et al. 1976). Indeed, such losses can be treated as a sequence of instantaneous small reductions of the energy, occurring during individual collision events with gas particles (and leading to the corresponding decrease of the Larmor radius). This treatment is justified since both the time and the length scales of the collision interactions are incomparably smaller than the respective gyration scales of a CR particle. The assumption of a negligible scattering is applicable to the ionization interactions, dominating the energy losses by nonrelativistic protons (see, e.g., Ginzburg & Syrovatskii 1964; Padovani et al. 2009). In the range of $10^5\ {\rm eV} \lesssim E \lesssim 5 \times 10^8\ {\rm eV}$, the ionization loss function is accurately approximated by

$$L(E) = L_*\left(\frac{E}{E_*}\right)^{-d}, \tag{9}$$

with $d \approx 0.82$, $L_* \approx 1.4 \times 10^{-14}\ {\rm eV\ cm^2}$ and $E_* = 10^5\ {\rm eV}$ (Padovani et al. 2018).

By multiplying Equation (8) with $L(E)$, we obtain a general solution $jL = \Psi(x + y)$. Here, Ψ is an arbitrary function with

$$x(\mu, s) = \int^s \frac{n_g(s')\ ds'}{\hat{\mu}(\mu_i, s')}; \quad y(E) = \int^E \frac{dE'}{L(E')}, \tag{10}$$

where $\mu_i(\mu, s) = \pm\sqrt{1 - (1 - \mu^2)/\tilde{B}(s)}$ is the inverse of Equation (4). This means that jL is conserved along lines of constant $x + y$. In this section, we are assuming a single-peaked magnetic field profile, as in Figure 1(b), and all quantities refer to forward-moving particles propagating toward the peak. Hence, the relation to the isotropic interstellar spectrum $j_i = vn_i$ is given by

$$j_+(\mu, E, s)L(E) = \frac{1}{2}j_i(E_i)L(E_i). \tag{11}$$

The relation between energy E_i at the cloud boundary and energy E at position s is obtained from Equation (10),

$$E_i^{1+d} = E^{1+d} + (1 + d)L_*E_*^dN_+. \tag{12}$$

The latter is determined by

$$N_+(\mu, s) = \int_0^s \frac{n_g(s')\ ds'}{\sqrt{1 - \tilde{b}(s', s)(1 - \mu^2)}}, \tag{13}$$

which is the actual column density traversed by a forward-moving particle on its helical trajectory, depending on $\tilde{b}(s', s) = B(s')/B(s) \leqslant 1$.

The ionization rate at position s due to forward-moving particles is

$$\zeta_+(s) = \int_0^1 d\mu \int_0^\infty j_+(\mu, E, s)\sigma_{\rm ion}(E)\ dE, \tag{14}$$

where $\sigma_{\rm ion}(E)$ is the ionization cross section. We notice that the mean energy ε lost by a CR particle per ionization event is practically independent of E (Padovani et al. 2009). This yields a simple relation,

$$L(E) \approx \varepsilon\sigma_{\rm ion}(E). \tag{15}$$

Therefore, we can use Equations (11), (14), and (15) to write

$$\zeta_+(s) = \frac{1}{2\varepsilon}\int_0^1 d\mu \int_0^\infty j_i(E_i)L(E_i)\ dE, \tag{16}$$

with $E_i(E, \mu, s)$ given by Equation (12).

To continue further, we generally need to assume an explicit form for $n_{\rm g}(s)$ and $B(s)$. However, we can also consider two limiting cases, which are determined by the behavior of $B(s)$ and provide exact lower and upper bounds on ζ_+. The *lower bound* (L) occurs when $\tilde{b}(s', s) = 1$ for $0 < s' < s$. In this case Equations (12), (13), and (16) show that ζ_+ is the same as if $B = B_i$ throughout the whole cloud. The *upper bound* (U) occurs if $\tilde{b}(s', s) = 0$ for $0 < s' < s$. In this case, the ionization rate due to forward-moving particles is increased relative to the constant-field case, because the CRs have accrued less column between $s' = 0$ and $s' = s$. Thus, the ionization rate by forward-moving particles is always limited in the range of

$$\zeta_{\rm L} \leqslant \zeta_+ \leqslant \zeta_{\rm U}.$$

Physically, the lower bound $\zeta_{\rm L}$ represents propagation of CRs along a constant magnetic field, where both the mirroring and focusing are absent, and therefore this is our *reference value* of the ionization rate. The upper bound $\zeta_{\rm U}$ reflects an extreme situation of all CRs having zero pitch angles. Hence, the relative increase of the ionization rate is conveniently quantified by the ratio $\mathcal{R} \equiv \zeta_+/\zeta_{\rm L}$, bounded between unity and $\zeta_{\rm U}/\zeta_{\rm L}$.

In order to calculate the value of $\mathcal{R}_{\rm max} = \zeta_{\rm U}/\zeta_{\rm L}$, let us consider a typical model spectrum of the interstellar CRs, approximately described by a power-law dependence for the nonrelativistic energy range (Ivlev et al. 2015),

$$j_i(E) = j_*\left(\frac{E}{E_*}\right)^{-a}. \tag{17}$$

We expect the results to be valid at column densities where Equation (9) is applicable, i.e., where all particles with $E_i \lesssim 10^5\ {\rm eV}$ have been attenuated, but particles with $E_i \gtrsim 5 \times 10^8\ {\rm eV}$ are not attenuated significantly. This corresponds to column densities of roughly 10^{19}–$10^{25}\ {\rm cm^{-2}}$ (Padovani et al. 2018).

If the value of the spectral index a is sufficiently small, $a < 1 - d \approx 0.2$, then the integral over E in Equation (16) is dominated by larger E. In practice, this means that $\zeta_+(s)$ remains approximately constant as long as the column density is smaller than the stopping range for $E \approx 5 \times 10^8$ eV, where a crossover to the relativistic spectrum $j_i \propto E^{-2.7}$ occurs (Ivlev et al. 2015). This stopping range nicely coincides with the upper limit of column densities where Equation (9) is still applicable. Therefore, attenuation of CRs with $a < 1 - d$ does not (substantially) affect the value of ζ_+ at column densities $\lesssim 10^{25}$ cm^{-2}, and effects of the mirroring and focusing for such interstellar spectra cancel out, as discussed in Section 2.

Thus, below we consider interstellar spectra with $a > 1 - d \approx 0.2$, for which the ionization at s is dominated by lower CR energies (viz., by the energies for which the stopping range is of the order of the column density at s). By substituting Equations (9), (12), and (17) in Equation (16), we obtain for the lower ionization bound (reference value)

$$\zeta_{\rm L}(s) = \int_0^1 K(\mu, s) d\mu, \tag{18}$$

where

$$K(\mu, s) = \frac{j_* L_*}{2\varepsilon} \times \int_0^\infty \left[\left(\frac{E}{E_*} \right)^{1+d} + (1+d) \frac{L_*}{E_*} \frac{N_{\rm eff}}{\mu} \right]^{-\frac{a+d}{1+d}} dE, \tag{19}$$

while for the upper bound we have

$$\zeta_{\rm U}(s) = K(1, s). \tag{20}$$

Here, $N_{\rm eff}(s) = \int_0^s n_g(s') ds'$ is the so-called *effective column density*, measured along a field line (see, e.g., Padovani et al. 2018). By making the substitution $E' = \mu^{\frac{1}{1+d}} E$ into Equation (19), one can easily show that

$$K(\mu, s) = \mu^{\frac{a+d-1}{1+d}} K(1, s). \tag{21}$$

Thus, performing the integration over μ in Equation (18), we find that $\zeta_{\rm U}/\zeta_{\rm L}$ does not depend on s and is equal to

$$\mathcal{R}_{\rm max} = 1 + \frac{a + d - 1}{1 + d}. \tag{22}$$

We conclude that, for any density profile and a single-peaked magnetic field, a combined effect of the mirroring and focusing is able to increase the ionization rate (relative to the reference value) by a factor no larger than $\mathcal{R}_{\rm max}$. For realistic values of the spectral index $a \lesssim 1$, we have $\mathcal{R}_{\rm max} \lesssim 1.5$; this factor naturally tends to unity when $a = 1 - d$.

Equation (22) becomes increasingly inaccurate above a column density of $\sim 10^{25}$ cm^{-2}, corresponding to the stopping range of CRs with energies where Equation (9) is no longer applicable.

3.2. Contribution of the Mirrored Particles

In the previous section, we only considered the ionization by incoming particles. Now we will estimate the contribution from the mirrored, backward-moving particles. We expect this to be less than the ionization rate by the forward-moving particles, because the mirrored particles have traveled through a larger column.

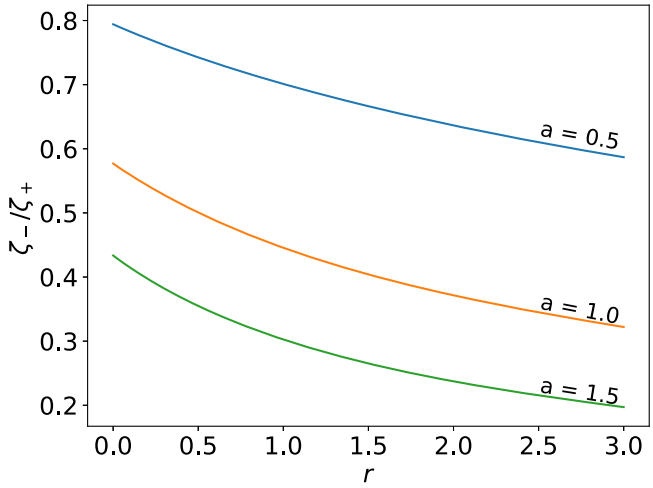

Figure 3. Ratio of ionization rates due to the mirrored (backward-moving) and forward-moving CRs, ζ_-/ζ_+, plotted vs. the parameter r, Equation (24). The curves represent different values of the spectral index a of interstellar CRs, Equation (17).

Let $\zeta_-(s)/\zeta_+(s)$ be a ratio of the ionization due to the mirrored particles to the ionization due to the forward-moving particles. Calculation of this ratio is difficult in general. To make the problem tractable and estimate the magnitude of the effect, we consider a model for the increase of magnetic field and gas density within the cloud, in which we let

$$\tilde{B}(s) = \left(\frac{s}{H} \right)^p; \quad n_g(s) = n_{g*} \left(\frac{s}{H} \right)^q, \tag{23}$$

with H being a relevant spatial scale and p and q positive. Even though Equation (23) yields an unphysical behavior of $B(s)$ for $s \lesssim H$, this region contributes negligibly compared to the region of interest ($s \gg H$), where the mirroring and focusing effects are strong. In the Appendix, we calculate $\zeta_+(s)$ and $\zeta_-(s)$ and demonstrate that their ratio does not depend on s, and is characterized by the spectral index a and the ratio

$$r = \frac{q + 1}{p} - 1. \tag{24}$$

Figure 3 shows ζ_-/ζ_+ as a function of r, plotted for different values of a. The behavior is easy to understand: it is a decreasing function, since larger r implies smaller p or larger q and hence more column between s and the mirror point (relative to the column between 0 and s). The constraint that p and q are positive means that $r > -1$; we have $r \to -1$ for a sharply increasing field (i.e., for a vanishing column between s and the mirror point), which implies $\zeta_- \to \zeta_+$. Larger values of a cause this decrease to happen more rapidly, as a harder spectrum means that the ionization rate falls off faster with increased column depth.

Under the assumption of magnetic flux freezing during the cloud collapse, we would expect $\frac{1}{2} \leqslant p/q \leqslant \frac{2}{3}$ (Crutcher 2012). Then we can write $r = r' + 1/p$, where $\frac{1}{2} \leqslant r' \leqslant 1$.

3.3. Ionization in Magnetic Pockets

As discussed in Section 2.2, the CR density can be drastically reduced at local field minima—magnetic pockets, where particles experience *defocusing* relative to the lower peak B_l, but the mirroring has no effect on their motion. This fact has profound implications for the ionization.

Let us first assume that the attenuation in a pocket is negligible compared to that in the cloud—we call such pockets "localized." The ionization rate by forward-moving particles, $\zeta_+^{\rm pock}$, can be calculated from Equation (16), where $\sqrt{1-B/B_l}$ is used for the lower limit of the integral over μ (see Section 2.2). The upper ionization bound, $\zeta_{\rm U}^{\rm pock}(s)$, for which we set $\tilde{b}=0$ in Equation (13), is readily obtained by following the same steps as in Section 3.1. This yields

$$\text{Localized:}\quad \frac{\zeta_{\rm U}^{\rm pock}}{\zeta_{\rm L}}=\mathcal{R}_{\rm max}\left(1-\sqrt{1-\frac{B}{B_l}}\right), \tag{25}$$

where the normalization is by the reference value $\zeta_{\rm L}$ and $\mathcal{R}_{\rm max}\equiv\zeta_{\rm U}/\zeta_{\rm L}$ is given by Equation (22). To derive the lower bound, representing the case of a constant field B_l outside the pocket, we notice that now $\tilde{b}=B_l/B\geqslant 1$. Substituting Equation (13) in Equation (16) and introducing a new variable $x=(1-\mu^2)B_l/B$, after simple transformations we obtain

$$\frac{\zeta_{\rm L}^{\rm pock}}{\zeta_{\rm L}}=\frac{1}{2}\mathcal{R}_{\rm max}\frac{B}{B_l}\int_0^1\frac{(1-x)^{\frac{1}{2}(\mathcal{R}_{\rm max}-1)}}{\sqrt{1-(B/B_l)x}}\,dx. \tag{26}$$

As expected, this yields $\zeta_{\rm L}^{\rm pock}\to\zeta_{\rm L}$ when $B\to B_l$; for deep regions in the pockets, where B/B_l is small, from Equations (25) and (26) we derive $\zeta_{\rm U}^{\rm pock}/\zeta_{\rm L}^{\rm pock}\approx\frac{1}{2}(\mathcal{R}_{\rm max}+1)$. The latter shows that the relative range of possible ionization rates in a (deep) pocket is half of that in the single-peaked case (Section 3.1).

Concerning the ionization by the mirrored particles, we notice that the value of ζ_-/ζ_+ is unaffected by the presence of a localized pocket, since the latter has largely the same effect on the pitch angle of both mirrored and forward-moving particles. Hence, their contribution can be evaluated using the results of Section 3.2.

We can also consider the opposite situation, where the column density of a magnetic pocket is much larger than that between the edge of the cloud and the pocket. When calculating the ionization rate by forward-moving particles in such "global" pockets, the column accrued exterior to the peak B_l can be ignored, i.e., one can assume that interstellar CRs directly enter the pocket. In this case, the lower ionization bound would be where the magnetic field in the pocket remains at the peak value B_l up to position s, where it drops to the value $B(s)$. This is physically equivalent to the lower bound derived for a localized pocket, and the ionization rate is therefore given by Equation (26). For the upper bound, we assume that the magnetic field in the pocket decreases from B_l to B right at s_l. The corresponding ionization rate can be derived from Equation (18) (which is the lower bound for the single-peaked field) where, again, the lower limit of integration is replaced with $\sqrt{1-B/B_l}$. We obtain that the ionization is reduced by a factor of

$$\text{Global:}\quad \frac{\zeta_{\rm U}^{\rm pock}}{\zeta_{\rm L}}=1-\left(1-\frac{B}{B_l}\right)^{\frac{1}{2}\mathcal{R}_{\rm max}}. \tag{27}$$

From Equations (26) and (27) it follows that the upper and lower ionization bounds in global pockets coincide when $B\to B_l$, and tend to the reference value $\zeta_{\rm L}$. The latter is easy to understand, since in this case CRs propagate along a quasi-constant magnetic field. In deep regions the difference between local and global pockets disappear and the upper-bound reduction factors, given by Equations (25) and (27), tend to the same value of $\zeta_{\rm U}^{\rm pock}/\zeta_{\rm L}\approx\frac{1}{2}\mathcal{R}_{\rm max}(B/B_l)\ll 1$. From Equation (26) we infer that the lower-bound reduction in this limit is a factor of $\frac{1}{2}(\mathcal{R}_{\rm max}+1)$ smaller.

The ionization by mirrored particles is reduced significantly in a global pocket. Indeed, forward-moving CRs entering the pocket from one side propagate without mirroring until (at least) the other side. A mirrored particle at a given position accrues on average the column density of the entire global pocket before returning back. Thus, the contribution of mirrored particles can be reasonably neglected.

4. Discussion and Conclusions

In order to draw general conclusions about the net effect of the magnetic mirroring and focusing, let us start with the single-peaked field profile, sketched in Figure 1(b), and consider two characteristic situations. One is when the ionization occurs sufficiently away from the center of a cloud, where $B(s)$ is still substantially smaller than the peak value B_p. CRs originating from the other side of the cloud are negligible in this case, both due to the strong attenuation and the narrow range of initial pitch angles that allow the particles to overcome the mirroring. Based on the results of Sections 3.1 and 3.2, we immediately obtain that the relative increase of the ionization rate with respect to the reference value $\zeta_{\rm L}$ (representing a constant field strength) is equal to $\mathcal{R}(1+\zeta_-/\zeta_+)$, where the upper bound for $\mathcal{R}$ is given by Equation (22) and the lower bound is unity. The other situation occurs near the cloud center, where the contribution of the mirrored particles is no longer important, and the ionization is due to CRs coming from both sides of the cloud. Then the relative increase of the ionization rate is simply $\mathcal{R}$. We have shown that for realistic values of the spectral index a, the total relative increase does not exceed a factor of 1.5–2.

In the presence of multiple magnetic peaks, illustrated in Figure 1(c), these conclusions remain unchanged everywhere except for the regions of local field minima—magnetic pockets, where the ionization can be decreased drastically. In Section 3.3, we show that the ionization decrease is described by a reduction factor for which we also consider two characteristic situations: localized pockets with column small compared to that between the pocket and the cloud edge, and the opposite situation of "global" pockets. In the former case, for practical purposes one can employ Equation (25) for the reduction factor; for global pockets, the reduction is given by Equation (27). For pockets with intermediate column densities it is not crucial which formula is used, since they differ at most by a factor of $\leqslant R_{\rm max}$.

Calculations of the ionization rate in dense molecular clouds and circumstellar disks inevitably contain significant uncertainties. These are primarily associated with poor knowledge of the gas distribution and the configuration of magnetic field lines in the cores, both leading in uncertainties in the effective column density $N_{\rm eff}$ and, hence, in the reference ionization rate $\zeta_{\rm L}(N_{\rm eff})$. The analysis presented above shows that, compared to these

uncertainties, the variations due to the CR mirroring and focusing are negligible and therefore can be safely neglected—as long as the field has a single-peaked profile. Within the magnetic pockets, the derived analytical formulas should be used to accurately calculate the relative decrease of the ionization rate in these regions.

The results of this paper were derived for effective column densities of up to $N_{\rm eff} \sim 10^{25}\,{\rm cm}^{-2}$. Remarkably, Padovani et al. (2018) have recently shown that at $N_{\rm eff} \gtrsim 3 \times 10^{25}\,{\rm cm}^{-2}$ the CR ionization is driven by indirect processes, mediated by secondary photons, and then the magnetic field plays no role at all. This allows us to conclude that the mirroring and focusing do not significantly affect the ionization outside the magnetic pockets at any column density.

We note that Padovani & Galli (2011) performed a numerical study of the CR mirroring and focusing for a specified density and magnetic field distribution, valid for a molecular cloud core in magnetostatic equilibrium. They also reached the conclusion that there was a near-cancellation of the magnetic mirroring and focusing terms. In detail, however, there appears to be a minor discrepancy with the present results—specifically, they find some reduction in the ionization rate due to the combined effect of mirroring and focusing, whereas we find a slight increase in the ionization rate. This discrepancy arises from their overestimate of the reduction of CR flux by mirroring (by the factor of $1-\sqrt{1-1/\tilde{B}}$ rather than $1/\tilde{B}$), and by their assumption that CRs lose all their kinetic energy in approaching the mirror point. The latter assumption was relaxed by Padovani et al. (2013), who studied the propagation of CRs along the magnetic field for a rotating collapsing core with different initial conditions (mass-to-flux ratio, angle between the mean magnetic field direction and the rotation axis). The severe reduction of the CR ionization rate, reported in this paper for certain regions, was attributed to the stronger effect of mirroring with respect to focusing. In fact, a preliminary analysis of their simulation data shows this strong reduction to be due to the presence of magnetic pockets, which is fully consistent with the results presented in Section 3.3.

To summarize, the effects of magnetic mirroring and focusing on the local CR density practically cancel each other out if there are no magnetic pockets. This implies that we can safely use available numerical results for CR ionization (calculated neglecting these magnetic effects) and simply assume the CR propagation along field lines. For situations where magnetic pockets are present, the ionization rate can be greatly reduced. We obtained simple expressions allowing accurate calculation of the ionization in localized or global pockets. In a separate paper, we plan to investigate conditions under which magnetic pockets may form, and study their effect on nonideal MHD processes occurring in dense cores and disks. Also, we will analyze the role of the CR diffusion along the magnetic field, caused by CR collisions with particles of the medium or by their (resonant and nonresonant) interaction with the fluctuating field.

M.P. acknowledges funding from the European Unions Horizon 2020 research and innovation programme under the Marie Skłodowska-Curie grant agreement No. 664931.

Appendix
Ionization Due to the Mirrored Particles

Let $N_+(\mu, s)$ and $N_-(\mu, s)$ be the column densities accrued at position s by, respectively, the forward-moving and mirrored particles having the local pitch-angle cosine of $\pm\mu$. The corresponding ionization rates $\zeta_+(s)$ and $\zeta_-(s)$ can be derived from Equation (16).

Substituting Equation (12) in Equation (16) and introducing new variable $E' = [(1+d)(L_*/E_*)N_\pm]^{-\frac{1}{1+d}}E$, we decouple $N_\pm$ from the resulting integrals over energy. For our purpose it is convenient to replace the integration over μ with the integration over μ_i, by using Equation (5). For locations in the cloud where $B(s) \gg B_i$ one can set $\mu_i \approx 1$ and $1-\mu_i^2 \approx \alpha_i^2$, so that $\mu \approx \pm\sqrt{1-\tilde{B}(s)\alpha_i^2}$. Using the initial energy spectrum (17), we obtain

$$\zeta_\pm(s) = T(s)\int_0^{1/\tilde{B}(s)} N_\pm^{1-\mathcal{R}_{\rm max}}\frac{d\alpha_i^2}{\sqrt{1-\tilde{B}(s)\alpha_i^2}}, \tag{28}$$

where $T(s)$ is a common pre-factor and $\mathcal{R}_{\rm max}$ is given by Equation (22). In the same approximation, from Equation (13) we obtain

$$N_+(\alpha_i, s) = \int_0^s \frac{n_g(s')\,ds'}{\sqrt{1-\tilde{B}(s')\alpha_i^2}}. \tag{29}$$

Then, we assume $\tilde{B}(s)$ and $n_g(s)$ to be given by Equation (23), and introduce $x = (s/H)^p\alpha_i^2$ and $x' = (s'/H)^p\alpha_i^2$. This yields

$$N_+ = \frac{n_{g*}H}{p\alpha_i^{2(r+1)}}\int_0^x \frac{x'^r\,dx'}{\sqrt{1-x'}}, \tag{30}$$

where $r = (q+1)/p - 1$. Similarly, we write

$$N_- = N_+ + \frac{2n_{g*}H}{p\alpha_i^{2(r+1)}}\int_x^1 \frac{x'^r\,dx'}{\sqrt{1-x'}}, \tag{31}$$

where we used the fact that $x' = 1$ is the mirror point. Finally, substituting Equations (30) and (31) in Equation (28), we derive

$$\zeta_+(s) = T'(s)\int_0^1\left[\frac{1}{x^{r+1}}\int_0^x\frac{x'^r\,dx'}{\sqrt{1-x'}}\right]^{1-\mathcal{R}_{\rm max}}\frac{dx}{\sqrt{1-x}}, \tag{32}$$

and

$$\zeta_-(s) = T'(s)\int_0^1\left[\frac{1}{x^{r+1}}\left(\int_0^x\frac{x'^r\,dx'}{\sqrt{1-x'}} + 2\int_x^1\frac{x'^r\,dx'}{\sqrt{1-x'}}\right)\right]^{1-\mathcal{R}_{\rm max}}\frac{dx}{\sqrt{1-x}}, \tag{33}$$

where $T'(s)$ is a (new) common pre-factor. We conclude that the ratio ζ_-/ζ_+ does not depend on s. The ratio is obviously smaller than unity (since $\mathcal{R}_{\rm max}(a) > 1$), and is a function of parameters r and a.

ORCID iDs

Kedron Silsbee https://orcid.org/0000-0003-1572-0505
Alexei V. Ivlev https://orcid.org/0000-0002-1590-1018
Marco Padovani https://orcid.org/0000-0003-2303-0096
Paola Caselli https://orcid.org/0000-0003-1481-7911

References

Allen, A., Li, Z.-Y., & Shu, F. H. 2003, ApJ, 599, 363
Cesarsky, C. J., & Völk, H. J. 1978, A&A, 70, 367
Chandran, B. D. G. 2000, ApJ, 529, 513
Chen, F. F. 1974, Introduction to Plasma Physics (New York: Plenum Press)
Crutcher, R. M. 2012, ARA&A, 50, 29
Desch, S. J., Connolly, H. C., Jr., & Srinivasan, G. 2004, ApJ, 602, 528
Ginzburg, V. L., & Syrovatskii, S. I. 1964, The Origin of Cosmic Rays (Oxford: Pergamon)
Ivlev, A. V., Dogiel, V. A., Chernyshov, D. O., et al. 2018, ApJ, 855, 23
Ivlev, A. V., Padovani, M., Galli, D., & Caselli, P. 2015, ApJ, 812, 135
Joos, M., Hennebelle, P., & Ciardi, A. 2012, A&A, 543, A128
Ko, C.-M. 1992, A&A, 259, 377
Lazarian, A. 2014, SSRv, 181, 1
Li, Z.-Y., Krasnopolsky, R., & Shang, H. 2013, ApJ, 774, 82
Mestel, L., & Spitzer, L., Jr. 1956, MNRAS, 116, 503
Morfill, G. E., Völk, H. J., & Lee, M. A. 1976, JGR, 81, 5841
Padoan, P., & Scalo, J. 2005, ApJL, 624, L97
Padovani, M., & Galli, D. 2011, A&A, 530, A109
Padovani, M., Galli, D., & Glassgold, A. E. 2009, A&A, 501, 619
Padovani, M., Hennebelle, P., & Galli, D. 2013, A&A, 560, A114
Padovani, M., Ivlev, A. V., Galli, D., & Caselli, P. 2018, A&A, 614, A111
Parker, E. N. 1963, Interplanetary Dynamical Processes (New York: Interscience)
Price, D. J., & Bate, M. R. 2008, MNRAS, 385, 1820
Skilling, J., & Strong, A. W. 1976, A&A, 53, 253
Yamamoto, S. 2017, Introduction to Astrochemistry: Chemical Evolution from Interstellar Clouds to Star and Planet Formation (Tokyo: Springer)
Zhao, B., Caselli, P., Li, Z.-Y., & Krasnopolsky, R. 2018, MNRAS, 473, 4868